jmr&t
Journal of Materials Research and Technology
www.jmrt.com.br

Review Article

Creep in amorphous metals☆

*Michael E. Kassner**, *Kamia Smith*, *Veronica Eliasson*

Department of Aerospace and Mechanical Engineering, University of Southern California, Los Angeles, United States

ARTICLE INFO

Article history:
Received 28 March 2014
Accepted 5 November 2014
Available online 2 January 2015

Keywords:
Bulk metallic glasses
Amorphous alloys
Creep
Time-dependent plasticity

ABSTRACT

This paper reviews the work on creep behavior of amorphous metals. There have been, over the past several years, a few reviews of the mechanical behavior of amorphous metals. Of these, the review of the creep properties of amorphous metals by Schuh et al. though oldest of the three, is particularly noteworthy and the reader is referred to this article published in 2007. The current review of creep of amorphous metals particularly focuses on those works since that review and places the work prior to 2007 in a different context where new developments warrant.

Michael E. Kassner graduated with a Bachelor in Science-Engineering from Northwestern University in 1972, and an MS and PhD in Materials Science and Engineering from Stanford University in 1979 and 1981. Kassner accepted a position at Lawrence Livermore National Laboratory in 1981 and was employed there until 1990 where he was Head of the Physical Metallurgy and Welding Section. He accepted a faculty position in the Mechanical Engineering Department at Oregon State University in 1990 where he was Northwest Aluminum Professor of Mechanical Engineering. He received the College of Engineering Outstanding Sustained Research Award in 1995. He moved in 2003 to accept a position as Chairman, Mechanical and Aerospace Engineering Department at the University of Southern California (USC). He is also a Professor of Materials Science at USC. He is currently Choong Hoon Cho Chair and Professor. He is currently active in pursuing research at USC on creep, fracture, fatigue and thermodynamics. Most recently, he was assigned to Washington, DC, as the Director of Research at the Office of Naval Research (ONR). He assumed the position in October 2009 until October 2012. He was responsible for overseeing the nearly one billion-dollar basic-research budget for the US Navy. He was awarded the Navy's Meritorious Public Service Medal for his tenure at ONR. He has published three books, one on the fundamentals of creep plasticity in metals, hot deformation of aluminum and aluminum alloys and another on phase diagrams and has authored or co-authored over 220 published articles. He is a Fellow of American Society of Metals (ASM), a Fellow of the American Society of Mechanical Engineers (ASME) and a Fellow of the American Association for the Advancement of Science (AAAS).

☆ Paper presented in the form of an abstract as part of the proceedings of the Pan American Materials Conference, São Paulo, Brazil, July 21st to 25th 2014.

* *Corresponding author.*

http://dx.doi.org/10.1016/j.jmrt.2014.11.003

Kamia Smith graduated from Wheaton College in Norton, Massachusetts in 2011 with a Bachelor of Arts degree in Chemistry. Smith then pursued graduate level studies at the University of Southern California. She completed her Masters of Science in Materials Science and Engineering in 2013 and is now currently pursuing her PhD in the same field. Her research, under Dr. Michael Kassner, studies the mechanical behaviors of materials under various stress conditions. During her first year as a doctorate student, Smith accepted a fellowship position in a program called Body Engineering Los Angeles GK-12. As a fellow, she worked in a Downtown Los Angeles middle school in which she taught her research to students in order to spark more engineering interest in younger generations. Smith looks to complete her studies by 2016.

Veronica Eliasson is an Assistant Professor at the Aerospace and Mechanical Engineering Department at University of Southern California. She graduated with a PhD in Mechanics from the Royal Institute of Technology, Sweden, in 2007 and then held a postdoctoral appointment until 2009 at the Graduate Aerospace Laboratories, California Institute of Technology. Her research interests are in the area of experimental mechanics with particular interest in high-speed visualization techniques.

1. Introduction

Amorphous metals are a relatively new class of alloy, originating in about 1960 with the discovery of thin metallic ribbons by splat cooling [1]. These are always alloys, and pure metal glasses have not yet been produced. As these alloys are non-crystalline, they have no dislocations, at least in the sense normally described in crystalline materials. Thus, amorphous metals have yield stresses that are higher than crystalline alloys. High fracture stress, low elastic moduli, and sometimes-favorable fracture toughnesses are observed. Often, favorable corrosion properties were observed, as well, partly due to an absence of grain boundaries. Towards 1990, alloys with deep eutectics were developed that allowed liquid structures to be retained in thicker sections in the amorphous state on cooling to ambient temperature [2–13]. With this development, there has been fairly intensive study of bulk metallic glasses (BMG) for possible structural applications. Most of the alloys in this chapter are relevant to BMGs. Table 1 lists some of the short-term mechanical properties of some BMGs taken from [14–34] and some of the impressive properties are listed.

Fig. 1, based on an illustration by [35], is a time–temperature-transformation (T–T-T) diagram that illustrates some of the important temperatures for metallic glasses. First, there is the equilibrium liquid to solid transition at the melting temperature T_m where, of course, multiple solid crystalline phases form on cooling. Below this temperature a T–T-T curve is illustrated. Cooling below T_m must be sufficiently rapid to avoid intersecting the "nose" of the curve. Also illustrated is the glass transition temperature, T_g.

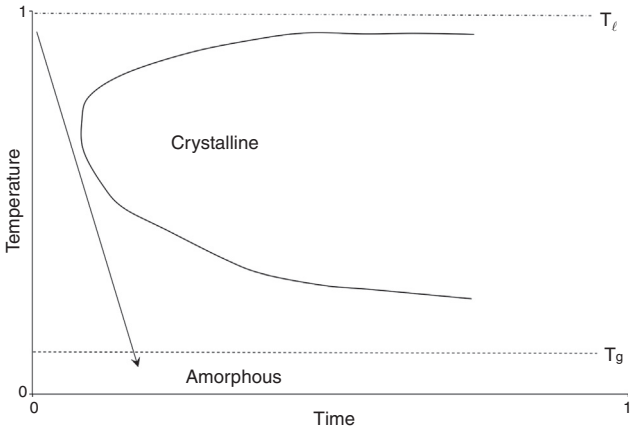

Fig. 1 – A time–temperature-transformation diagram that illustrates the important temperature regions of BMGs from Ref. [36].

This is generally assigned to that temperature where there is discontinuity in the change of a property (e.g. heat capacity, thermal expansion coefficient, etc.) with temperature. The region between T_m and T_g is generally referred to as the supercooled liquid regime. Some values for various BMGs are listed in Table 2 [36–47].

The discussions in this chapter will be largely confined to temperatures above 0.7 T_g. As will be discussed subsequently, this is the regime in which homogeneous deformation is observed. This review refers to this regime as a "creep regime" of amorphous metals. A practical importance of this regime is that this is where forming of a metallic glass is frequently performed. This regime is contrasted by the regime of lower temperatures where heterogeneous deformation or shear banding is often (but not always) observed.

2. Mechanisms of deformation

2.1. *Overview*

The suggested deformation mechanism has generally fallen into three categories: (a) Dislocation-like defects [48–50], (b) diffusion-type deformation [51], and (c) shear transformation zones (STZs) [52,53]. These are illustrated in Fig. 2, and are all early explanations for plasticity, but it appears that the amorphous metals community has generally embraced the third, STZ [12,13,54].

The essence of this latter mechanism is that there is a so-called "free volume" in amorphous metals. Free volume is a "concept" and it has no absolute definition. The starting state is the baseline; only the difference has meaning, so a change in density after deformation defines the free volume. The exact form and shape of these free volumes is not known. Increasing free volume would be associated with decreased density. Estimates for free volume for $Zr_{41.2}Ti_{13.8}Cu_{12.5}Ni_{10}Be_{22.5}$ (Vitreloy 1) is about 3% [54]. Free volume decreases (tighter packing) appear to increase ductility in homogeneous deformation

Table 1 – Mechanical properties of some glassy alloys from Ref. [13].

Material	E (GPa)	σ_y (MPa)	σ_f (MPa)	ε_y (%)	ε_p (%)	References
$Co_{43}Fe_{20}Ta_{5.5}B_{31.5}$	268		5185	2		[14]
$Cu_{60}Hf_{25}Ti_{15}$	124	2024	2088		1.6	[15]
$(Cu_{60}Hf_{25}Ti_{15})_{96}Nb_4$	130		2405		2.8	[16]
$Cu_{47}Ti_{33}Zr_{11}Ni_6Sn_2Si_1$		1930	2250			[17]
$Cu_{50}Zr_{50}$	84	1272	1794	1.7	6.2	[18]
$Cu_{64}Zr_{36}$	92.3		2000	2.2		[19]
$(Fe_{0.9}Co_{0.1})_{64.5}Mo_{14}C_{15}B_6Er_{0.5}$	192	3700	4100		0.55	[20]
$Fe_{71}Nb_6B_{23}$			4850		1.6	[21]
$Fe_{72}Si_4B_{20}Nb_4$	200		4200	2.1	1.9	[22]
$Fe_{74}Mo_6P_{10}C_{7.5}B_{2.5}$		3330	3400		2.2	[23]
$[(Fe_{0.6}Co_{0.4})_{0.75}B_{0.2}Si_{0.05}]_{96}Nb_4$	210	4100	4250	2	2.25	[24]
$Fe_{49}Cr_{15}Mo_{14}C_{15}B_6Er_1$	220	3750	4140		0.25	[25]
$Gd_{60}Co_{15}Al_{25}$	70		1380		1.97	[26]
$Ni_{61}Zr_{22}Nb_7Al_4Ta_6$			3080		5	[27]
$Pd_{77.5}Cu_6Si_{16.5}$		1476	1600		11.4	[28]
$Pd_{79}Cu_6Si_{10}P_5$	82	1475	1575		3.5	[29]
$Pt_{57.5}Cu_{14.7}Ni_{5.3}P_{22.5}$		1400	1470	2	20	[30]
$Ti_{41.5}Zr_{2.5}Hf_5Cu_{42.5}Ni_{7.5}Si_1$	95		2040		0	[31]
$Zr_{55}Cu_{20}Al_{20}Ni_5$		1410	1420			[32]
$Zr_{41.25}Ti_{13.75}Cu_{12.5}Ni_{10}Be_{22.5}$	96	1900	1900	2		[33]
$Zr_{57}Nb_5Al_{10}Cu_{15.4}Ni_{12.6}$	86.7	1800	1800	2		[34]

Note: E, Young's modulus; σ_y, yield strength; σ_f, fracture stress; ε_y, elongation at yielding; ε_p, plastic elongation. All the tests were conducted under compression, generally, at strain-rates from $(1–5) \times 10^{-4}\ s^{-1}$.

Table 2 – Deformation data of some BMGs in the super-cooled liquid region from Ref. [78].

Alloys (in at%)	T_g (K)	T_x (K)	*m* value	Ductility[a]	References
$La_{55}Al_{25}Ni_{20}$	480	520	1.0	1800 (T)	[36]
$Zr_{65}Al_{10}Ni_{10}Cu_{15}$	652	757	0.8–1.0	340 (T)	[37]
$Zr_{52.5}Al_{10}Ti_5Cu_{17.9}Ni_{14.6}$	358	456	0.45–0.55	650 (T)	[38]
$Zr_{55}Cu_{30}Al_{10}Ni_5$	683	763	0.5–1.0	N/A (C)	[39]
$La_{60}Al_{20}Ni_{10}Co_5Cu_5$	451	523	1.0	N/A	[40]
$Pd_{40}Ni_{40}P_{20}$	589	670	0.5–1.0	0.94 (C)	[41]
$Zr_{65}Al_{10}Ni_{10}Cu_{15}$	652	757	0.83	750 (T)	[42]
$Zr_{55}Al_{10}Cu_{30}Ni_5$	670	768	0.5–0.9	800 (T)	[43]
$Ti_{45}Zr_{24}Ni_7Cu_8Be_{16}$	601	648	N/A	1.0 (T)	[44]
$Cu_{60}Zr_{20}Hf_{10}Ti_{10}$	721	766	0.3–0.61	0.78 (C)	[45]
$Zr_{52.5}Al_{10}Cu_{22}Ti_{2.5}Ni_{13}$	659	761	0.5–1.0	>1.0 (C)	[46]
$Zr_{41.25}Ti_{13.75}Ni_{10}Cu_{12.5}Be_{22.5}$	614	698	0.4–1.0	1624 (T)	[47]

[a] "T" and "C" stand for tension and compression, respectively.

at ambient temperature [55]. With an applied stress, groups of atoms (e.g. few to 100 [2,54,56]), under an applied shear stress, τ, move and perform work. This constitutes an STZ. Argon et al. [51,52] considered that the STZ operation takes place within the elastic confinement of a surrounding glass matrix, and the shear distortion leads to stress and strain redistribution around the STZ region [2,51,52]. When the STZs exist throughout the alloy we have homogeneous deformation. STZs also occur in shear bands leading to heterogeneous deformation. STZs have been observed to create free volume during homogeneous deformation [57,58]. Steady-state flow within the homogeneous regime can be considered a case where there is a balance between free volume creation and annihilation [77].

Fig. 2b illustrates the STZ mechanism. Argon et al. described the activation energy for this process and Schuh et al. estimated the predicted activation energy, Q, as 100–500 kJ/mol. Table 3 [52,56,59,60] lists some of the experimentally observed activation energies which are consistent with Argon's predictions.

Table 3 – Activation energies for creep of selected metallic glasses ([6,52,56,59]).

Composition	T_g (K)	T_{test} (K)	ΔQ (kJ/mol)
$Al_{20}Cu_{25}Zr_{55}$	740	573	230.12
$Cu_{40}Zr_{60}$	677	543	218.82
$Cu_{56}Zr_{44}$	727	573	217.57
$Cu_{60}Zr_{40}$	750	573	228.45
$Pd_{80}Si_{20}$	673	546	191.63
$Zr_{55}Cu_{30}Al_{10}Ni_5$			410
$Au_{49}Ag_{5.5}Pd_{2.3}Cu_{26.9}Si_{16.3}$			103
$Zr_{44}Ti_{11}Cu_{10}Ni_{10}Be_{25}$	625/632		366

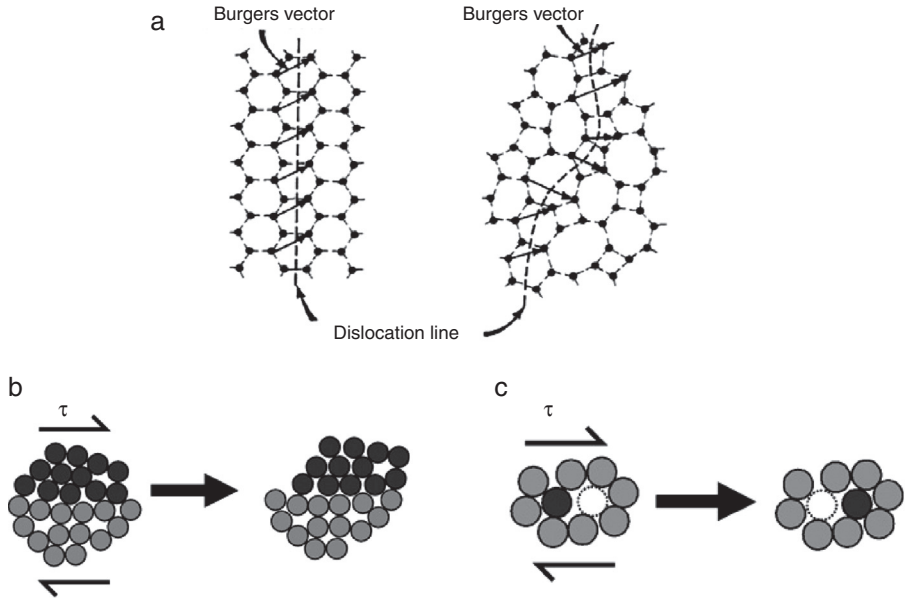

Fig. 2 – (a) Two-dimensional representation of a dislocation line in crystalline (left) and amorphous (right) solids, atomistic deformation of amorphous metals in the form of (b). Shear transformation zones (STZ), and (c). Local atomic jump. Figure adapted from [12].

The equations that have been used to describe the creep-rate based on STZ have used the classic rate equation formalism leading to [2]:

$$\dot{\gamma} = \alpha_o \nu_o \gamma_o \cdot \exp\left(-\frac{Q}{kT}\right) \sinh\left(\frac{\tau V}{kT}\right), \quad (1)$$

where α_O is a constant that includes the fraction of material deforming by activation, ν_O is an attempt frequency, and γ_O is the characteristic strain of an STZ, and V is the activation volume. The hyperbolic sine function arises, as there can be both a forward and reverse "reaction".

At low stresses ($\tau \ll kT/V$), this equation reduces to the Newtonian:

$$\dot{\gamma} = \frac{\alpha_o \nu_o \gamma_o V}{kT} \cdot \exp\left(-\frac{Q}{kT}\right) \tau, \quad (2)$$

since "reverse" deformation is irrelevant.

Conversely, at stresses, $\tau \gg kt/V$,

$$\dot{\gamma} = \frac{1}{2}\alpha_o \nu_o \gamma_o \cdot \exp\left(-\frac{Q - \tau V}{kT}\right), \quad (3)$$

Schuh et al. [2] point out that Eq. (1) suggests a Newtonian region followed by, with increasing stress, continual increase in stress exponent. Examples of BMGs that have evinced Eqs. (1)–(3) behaviors are illustrated in Figs. 3 and 4, which plot the steady-state creep behavior of several BMGs [2,36].

The figures on steady-state behavior illustrate that with increasing strain-rate and/or decreasing temperature there is a breakdown in Newtonian behavior and the apparent stress-exponent increases. Generally, this has been regarded as a natural consequence of Eq. (2), the rate equation that predicts Newtonian behavior at low stresses (higher temperature and lower strain-rates) but increased exponents with higher stresses (low temperatures and higher strain-rates). This explanation does not appear to be unanimously embraced [36]. For some, an important question is whether the non-Newtonian homogeneous deformation region is actually a reflection of nano-crystallization.

These equations suggest that free volume is largely responsible for plastic flow; larger free volumes would appear to more easily lead to regions of plastic flow. Schuh et al. point out that atomic simulations have suggested that other variables such as short-range chemical ordering can affect plasticity as well, which is not explicitly included in the above equations [61–64]. The pressure sensitivity of these equations was addressed by Sun et al. [65].

Nieh and Wadsworth [36] found that nano-crystallization occurred in $Zr_{10}Al_5Ti_{19.9}Cu_{14.6}Ni$ BMG coincident with the deviation from Newtonian behavior. Nieh rationalized the nano-crystalline precipitates as akin to dispersion strengthening. Suryanarayana and Inoue [66] appear to suggest that the stress exponent increases due to second phase strengthening of the nanoparticles by a straightforward rule of mixtures for the flow strength. Schuh et al. [2] referenced the Nieh and Wadsworth work and certainly acknowledged the observation that deformation can induce crystallization (as have others [66–69]) but appear to favor the rate equation as an explanation for the deviation from Newtonian behavior at higher stresses. Wang et al. [70] found only non-linear creep behavior in Vitreloy 1 if some crystallization occurred. Whereas Newtonian conditions led to elongations in $La_{55}Al_{25}Ni_{20}$ in excess of 20,000% [36], those at higher rates with non-Newtonian behavior exhibited dramatically reduced values. Many authors [2,12,13] proposed metallic glass deformation maps, similar to the construct by Ashby and Frost for crystalline materials. A metallic glass deformation–map is illustrated in Fig. 5.

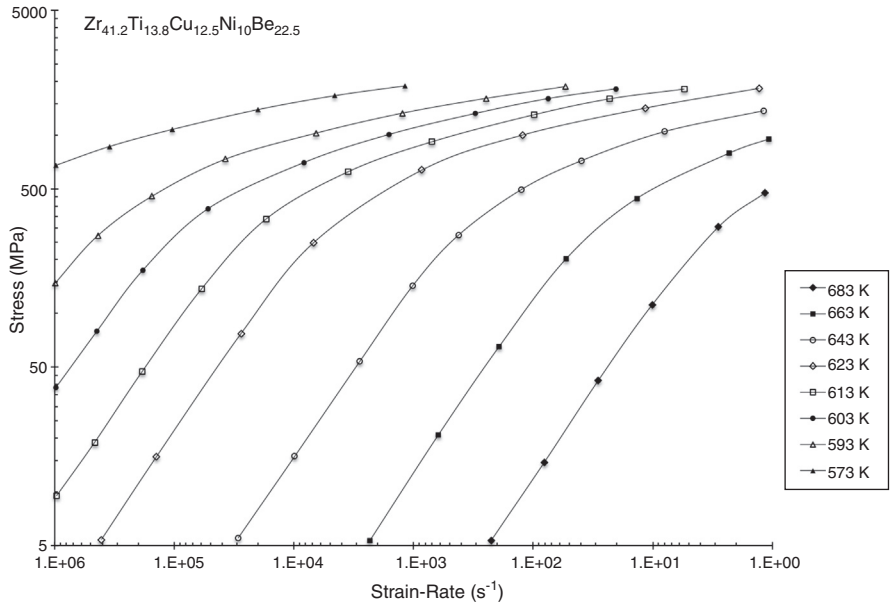

Fig. 3 – Steady-state homogeneous flow data for $Zr_{41.2}Ti_{13.8}Cu_{12.5}Ni_{10}Be_{22.5}$ metallic glass at elevated temperatures, from the work of Lu et al. [53].
Figure based on [2].

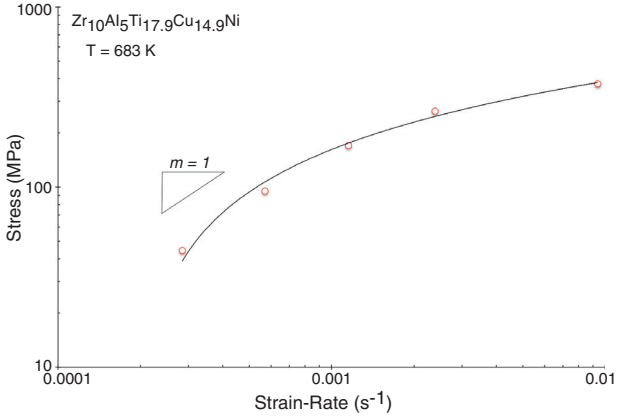

Fig. 4 – Stress–strain rate curve for a $Zr_{10}Al_5Ti_{17.9}Cu_{14.6}Ni$ glassy alloy shows Newtonian flow at low strain rates but non-Newtonian at high strain rates (data from Ref. [37]).
Figure based on [36].

Newtonian deformation appears to reflect a fully amorphous alloy, but at least in other regions, including heterogeneous deformation, nano-crystallization may be occurring [66–69].

Furthermore, as will be discussed in a subsequent section, homogeneous deformation may extend to low temperature, in at least some cases.

2.2. *Homogeneous flow at very low temperatures*

Recent work [57,71–73] shows that, given sufficient time, homogeneous deformation can be detected under "electrostatic" (i.e. at a stress less than the yield stress, σ_y) loading at room temperature (RT). The stress exponent was not assessed, so it was unclear whether Newtonian flow was observed. Alloys include $Zr_{46.75}Ti_{8.25}Cu_{7.5}Ni_{10}Be_{27.5}$, $Ni_{62}Nb_{38}$, $Cu_{50}Zr_{50}$, $Cu_{57}Zr_{43}$ and $Cu_{65}Zr_{35}$. Of course, some BMGs, such as $Zn_{20}Cu_{20}Tb_{20}(Li_{0.55}Mg_{0.45})_{20}$, may have low T_g (323 K) allowing homogeneous deformation at RT [74]. Alloys with higher packing densities exhibit greater plastic strain during homogeneous deformation at room temperature, but show less global plasticity during inhomogeneous deformation in a typical compression test [55]. Park et al. [57] suggest deformation induced structural disordering by molecular dynamic simulations, although others [73] imply STZ as the mechanism. Compression tests on $Pd_{77}Si_{23}$ with cylindrical samples of diameters 8 μm and 140 nm showed that as the sample size decreased to the submicron range, homogeneous deformation occurs and was suggested to occur due to the necessity of a critical size volume for shear bands [75]. Similar results were noted by others [76].

2.3. *Anelasticity*

In the above discussion of the so-called "electrostatic" regime, a substantial fraction of the (small) non-elastic strain is anelastic. It should be noted that the STZ model naturally predicts some anelasticity. An isolated STZ, by the Argon model, is elastically constrained during activation. This implies that even at a low applied stress (where backflow, according to Eq. (2), is negligible), there is, nonetheless, a back stress that on unloading leads to anelastic back flow. It was additionally pointed out by Ke et al. [72] that there is a range of atomic environments in a glass such that some atoms reside in regions where the local topology is unstable. In these regions, the response to shear stress may include not only atomic displacements but also an anelastic reshuffling of the atomic near-neighbors (i.e. an anelastic STZ operation). Even though

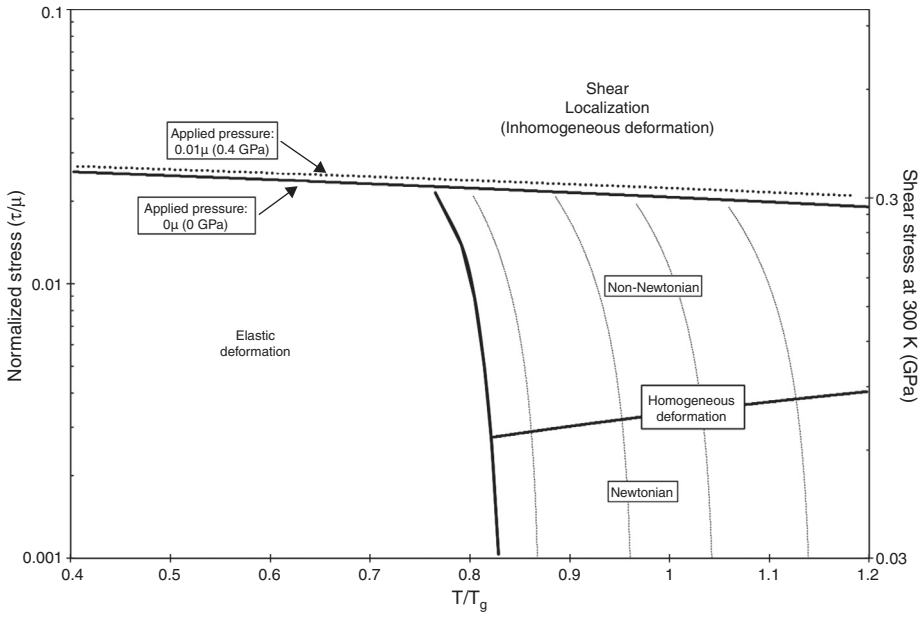

Fig. 5 – Deformation mechanism maps for metallic glass plotted in (a) normalized stress versus normalized temperature. The absolute stress values indicated in the figure are for the $Zr_{41.2}Ti_{13.8}Cu_{12.5}Ni_{10}Be_{22.5}$ metallic glass. Adapted from [2,12].

the fraction of atoms involved in these events may be small, the local strains are large enough that their cumulative effect makes a significant contribution to the macroscopic strain [72].

2.4. *Primary and transient creep (non-steady-state flow)*

Steady-state flow has principally been discussed. So far, it has been presumed that STZs create free volume (leading to softening) and that recovery processes involve the annihilation of free volume (leading to hardening). Therefore, steady state has been regarded as a balance between free volume creation and annihilations. Other hardening effects such as chemical ordering have not been explicitly considered for steady state. It has been suggested that there can be a net free volume increase or decrease during deformation that precedes a steady state. Fig. 6 from Lu et al. [53] shows hardening at the onset of deformation that continues beyond the eventual steady state. The interpretation of this peak stress followed by softening to a steady state is unclear.

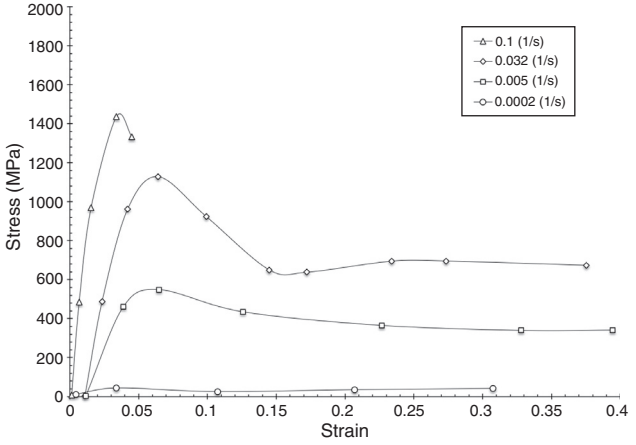

Fig. 6 – Effect of strain rate on the uniaxial stress–strain behavior of Vitreloy 1 at 643 K and strain rates of 1.0 × 10−1, 3.2 × 10−2, 5.0 × 10−3 and 2.0 × 10−4 s−1 [55].

3. Summary

This review of creep (above 0.7 T_g) in amorphous alloys emphasizes a variety of conclusions. First, the mechanism of creep appears to largely be explained by shear transformation zones where deformation is homogeneous. The descriptive equation for STZs suggests a Newtonian region followed by, with increasing stress, a continual increase in the stress exponent. It is not clear, as some suggest, that the non-Newtonian behavior is due to nano-crystallization. Second, homogeneous deformation at room temperature has recently been observed. Third, a substantial fraction of the small non-elastic strain at room temperature is anelastic. Fourth, during primary creep, STZs create free volume, leading to softening. Furthermore, recovery processes or annihilation of free volume leads to hardening.

Conflicts of interest

The authors declare no conflicts of interest.

Acknowledgment

Support by the US Defense Threat Reduction Agency under grant HDTRA1-11-1-0067 is appreciated.

REFERENCES

[1] Klement W, Willens RH, Duwez P. Non-crystalline structure in solidified gold-silicon alloys. Nature 1960;187:869.
[2] Schuh CA, Hufnagel TC, Ramamurty U. Mechanical behavior of amorphous alloys. Acta Mater 2007;55:4067–109.
[3] Kui HW, Greer AL, Turnbull D. Formation of bulk metallic glass by fluxing. Appl Phys Lett 1984;45:615–6.
[4] Nishiyama N, Inoue A. Glass-forming ability of bulk $Pd_{40}Ni_{10}Cu_{30}P_{20}$ alloy. Jpn Inst Metals Mater: Mater Trans 1996;37:1531–9.
[5] Lu IR, Wilde G, Görler GP, Willnecker R. Thermodynamic properties of Pd-based glass-forming alloys. J Non-Cryst Solids 1999;250-2:577–81.
[6] Inoue A, Yamaguchi H, Zhang T, Masumoto T. Al–La–Cu amorphous alloys with a wide supercooled liquid region. Jpn Inst Metals Mater: Mater Trans 1990;31:104–9.
[7] Inoue A, Zhang T, Masumoto T. Zr–Al–Ni amorphous-alloys with high glass-transition temperature and significant supercooled liquid region. Jpn Inst Metals Mater: Mater Trans 1990;31(3):177–83.
[8] Peker A, Johnson WL. A highly processable metallic glass: $Zr_{41.2}Ti_{13.8}Cu_{12.5}Ni_{10,0}Be_{22.5}$. Appl Phys Lett 1993;63(17):2342–4.
[9] Schroers J, Johnson WL. Highly processable bulk metallic glass-forming alloys in the Pt–Co–Ni–Cu–P system. Appl Phys Lett 2004;84(18):3666–8.
[10] Ponnambalam V, Poon SJ, Shiftlet GJ. Fe-based bulk metallic glasses with diameter thickness larger than one centimeter. J Mater Res 2004;19(5):1320–3.
[11] Lu ZP, Liu CT, Thompson JR, Porter WD. Structural amorphous steels. Phys Rev Lett 2004;92(24):245503.
[12] Trexler MM, Thandani N. Mechanical properties of bulk metallic glasses. Prog Mater Sci 2010;55:759–839.
[13] Suryanarayana C, Inoue A. Bulk Metallic Glasses. Boca Raton: CRC Press, Taylor and Francis Group; 2011.
[14] Inoue A, Shen BL, Koshiba H, Kato H, Yavari AR. Cobalt-based bulk glassy alloy with ultrahigh strength and soft magnetic properties. Nat Mater 2003;2:661–3.
[15] Qin CL, Zhang W, Asami K, Kimura HM, Wang XM, Inoue A. A novel Cu-based BMG composite with high corrosion resistance and excellent mechanical properties. Acta Mater 2006;54(14):3713–9.
[16] Qin CL, Zhang W, Asami K, Ohtsu N, Inoue A. Glass formation, corrosion behavior and mechanical properties of bulk glassy Cu–Hf–Ti–Nb alloys. Acta Mater 2005;53: 3903–11.
[17] Fu HM, Zhang HF, Wang H, Zhang QS, Hu ZQ. Synthesis and mechanical properties of Cu-based bulk metallic glass composites containing in-situ TiC particles. Scripta Mater 2005;52:669–73.
[18] Das J, Tang MB, Kim KB, Theissmann R, Baier F, Wang WH, et al. 'Work Hardenable' ductile bulk metallic glass. Phys Rev Lett 2005;94, 205501-1–205501-4.
[19] Xu DH, Lohwongwatana B, Duan G, Johnson WL, Garland C. Bulk metallic glass formation in binary Cu-rich alloy series – $Cu_{100-x}Zr_x$ ($x = 34$, 36, 38.2, 40 at.%) and mechanical properties of bulk $Cu_{64}Zr_{36}$ glass. Acta Mater 2004;52: 2621–4.
[20] Gu XJ, Poon SJ, Shiflet GJ. Mechanical properties of iron-based bulk metallic glasses. J Mater Res 2007;22:344–51.
[21] Yao JH, Wang JQ, Li Y. Ductile Fe–Nb–B bulk metallic glass with ultrahigh strength. Appl Phys Lett 2008;92, 251906-1–251906-3.
[22] Amiya K, Urata A, Nishiyama N, Inoue A. Fe–B–Si–Nb bulk metallic glasses with high strength above 4000 MPa and distinct plastic elongation. Mater Trans 2004;45(4):1214–8.
[23] Liu FJ, Yang QW, Pang SJ, Ma CL, Zhang T. Ductile Fe-based BMGs with high glass forming ability and high strength. Mater Trans 2008;49:231–4.
[24] Inoue A, Shen BL, Chang CT. Super-high strength of over 4000 MPa for Fe-based bulk glassy alloys in $[(Fe_{1-x}Co_x)_{0.75}B_{0.2}Si_{0.05}]_{96}Nb_4$ system. Acta Mater 2004;52(14):4093–9.
[25] Gu XJ, Poon SJ, Shiflet GJ. Effects of carbon content on the mechanical properties of amorphous steel alloys. Scripta Mater 2007;57(4):289–92.
[26] Chen D, Takeuchi A, Inoue A. Gd–Co–Al and Gd–Ni–Al bulk metallic glasses with high glass forming ability and good mechanical properties. Mater Sci Eng A 2007;457:226–30.
[27] Na JH, Park JM, Han KH, Park BJ, Kim WT, Kim DH. The effect of Ta addition on the glass forming ability and mechanical properties of Ni–Zr–Nb–Al metallic glass alloys. Mater Sci Eng A 2006;431:306–10.
[28] Yao KF, Yang YQ, Chen B. Mechanical properties of Pd–Cu–Si bulk metallic glass. Intermetallics 2007;15:639–43.
[29] Liu L, Inoue A, Zhang T. Formation of bulk Pd–Cu–Si–P glass with good mechanical properties. Mater Trans 2005;46:376–8.
[30] Schroers J, Johnson WL. Ductile bulk metallic glasses. Phys Rev Lett 2004;93, 255506-1–255506-4.
[31] Ma CL, Soejima H, Ishihara S, Amiya K, Nishiyama N, Inoue A. New Ti-based bulk glassy alloys with high glass-forming ability and superior mechanical properties. Mater Trans 2004;45:3223–7.
[32] Xie GQ, Louzguine-Luzgin DV, Kimura HM, Inoue A. Ceramic particulate reinforced $Zr_{55}Cu_{30}Al_{10}Ni_5$ metallic glassy matrix composite fabricated by spark plasma sintering. Mater Trans 2007;48:1600–4.
[33] Conner RD, Dandliker RB, Johnson WL. Mechanical properties of tungsten and steel fiber reinforced $Zr_{41.25}Ti_{13.75}Cu_{12.5}Ni_{10}Be_{22.5}$ metallic glass matrix composites. Acta Metal 1998;46(17):6089–102.
[34] Choi-Yim H, Conner RD, Szuecs F, Johnson WL. Processing, microstructure and properties of ductile metal particulate reinforced $Zr_{57}Nb_5Al_{10}Cu_{15.4}Ni_{12.6}$ bulk metallic glass composites. Acta Mater 2002;50:2737–45.
[35] Schroers J. The superplastic forming of bulk metallic glasses. J Metals 2005;57(5):35–9.
[36] Nieh TG, Wadsworth J. Homogeneous deformation of bulk metallic glasses. Scripta Mater 2006;55:387–92.
[37] Kawamura Y, Nakamura T, Inoue A. Superplasticity in $Pd_{40}Ni_{40}P_{20}$ metallic glass. Scripta Mater 1998;39(3):301–6.
[38] Nieh TG, Mukai T, Liu CT, Wadsworth J. Superplastic behavior of a Zr–10Al–5Ti–17.9Cu–14.6Ni metallic glass in the supercooled liquid region. Scripta Mater 1999;40(9):1021–7.
[39] Reger-Leonhard A, Heilmaier M, Eckert J. Newtonian flow of $Zr_{55}Cu_{30}Al_{10}Ni_5$ bulk metallic glassy alloys. Scripta Mater 2000;43(5):459–64.
[40] Saotome Y, Hatori T, Zhang T, Inoue A. Superplastic micro/nano-formability of $La_{60}Al_{20}Ni_{10}Co_5Cu_5$ amorphous alloy in supercooled liquid state. Mater Sci Eng A 2001;304:716–20.
[41] Chu JP, Chiang CL, Nieh TG, Kawamura Y. Superplasticity in a bulk amorphous Pd–40Ni–20P alloy: a compression study. Intermetallics 2002;10(11):1191–5.
[42] Kim WJ, Ma DS, Jeong HG. Superplastic flow in a $Zr_{65}Al_{10}Ni_{10}Cu_{15}$ metallic glass crystallized during deformation in a supercooled liquid region. Scripta Mater 2003;49(11):1067–73.

[43] Chu JP, Chiang CL, Mahalingam T, Nieh TG. Plastic flow and tensile ductility of a bulk amorphous $Zr_{55}Al_{10}Cu_{30}Ni_5$ alloy at 700 K. Scripta Mater 2003;49(5):435–40.
[44] Bae DH, Park JM, Na JH, Kim DH, Kim YC, Lee JK. Deformation behavior of Ti–Zr–Ni–Cu–Be metallic glass and composite in the supercooled liquid region. J Mater Res 2004;19(3):937–42.
[45] Chiang CL, Chu JP, Lo CT, Wang ZX, Wang WH, Wang JG, et al. Homogeneous plastic deformation in a Cu-based bulk amorphous alloy. Intermetallics 2004;12:1057–61.
[46] Bletry M, Guyot P, Brechet Y, Blandin JJ, Soubeyroux JL. Homogeneous deformation of bulk metallic glasses in the supercooled liquid state. Mater Sci Eng A 2004;387–389:1005–11.
[47] Wang G, Shen J, Sun JF, Huang YJ, Zou J, Lu ZP, et al. Superplasticity and superplastic forming ability of a Zr–Ti–Ni–Cu–Be bulk metallic glass in the supercooled liquid region. J Non-Cryst Solids 2005;351(81):209–17.
[48] Gilman JJ. Flow via dislocations in ideal glasses. J Appl Phys 1973;44(2):675–9.
[49] Li JCM. Chapter 9: Micro-mechanisms of deformation and fracture. In: Gilman JJ, Leamy HJ, editors. Metallic glasses. Materials Park, OH: American Society for Metals; 1978.
[50] Spaepen F. A microscopic mechanism for steady state inhomogeneous flow in metallic glasses. Acta Metal 1977;25:407–15.
[51] Argon AS. Plastic deformation in metallic glasses. Acta Metal 1979;27(1):47–58.
[52] Argon AS, Shi LT. Development of visco-plastic deformation in metallic glasses. Acta Metal 1983;31:499–507.
[53] Lu J, Ravichandran G, Johnson WL. Deformation behavior of the $Zr_{41.2}Ti_{13.8}Cu_{12.5}Ni_{10}Be_{22.5}$ bulk metallic glass over a wide range of strain-rates and temperatures. Acta Mater 2003;51:3429–43.
[54] Masuhr A, Busch R, Johnson WL. Thermodynamics and kinetics of the $Zr_{41.2}Ti_{13.8}Cu_{10.0}Ni_{12.5}Be_{22.5}$ bulk metallic glass forming liquid: glass formation from a strong liquid. J Non-Cryst Solids 1999;250–252(1):566–71.
[55] Park KW, Lee CM, Fleury E, Lee JC. Plasticity of amorphous alloys assessed by their homogeneous flow rate. Scripta Mater 2009;61:363–6.
[56] Song SX, Lai YH, Huang JC, Nieh TG. Homogeneous deformation of Au-based metallic glass micropillars in compression at elevated temperatures. Appl Phys Lett 2009;94:061911.
[57] Park KW, Lee CM, Wakeda M, Shibutani Y, Falk ML, Lee JC. Elastically induced structural disordering in amorphous alloys. Acta Mater 2008;56:5440–50.
[58] De Hey P, Sietsma J, Van Den Beukel A. Structural disordering in amorphous $Pd_{40}Ni_{40}P_{20}$ induced by high temperature deformation. Acta Mater 1998;46:5873–82.
[59] Fátay D, Gubicza J, Lendvai J. Indentation creep behavior of a Zr-based bulk metallic glass. J Alloys Compd 2007;75:434–5.
[60] Daniel BSS, Heilmaier M, Reger-Leonhard A, Eckert J, Schultz L. On the high temperature creep and relaxation behaviour of Zr-based bulk metallic glasses. In: Inoue A, Yavari AR, Johnson WL, Dauskardt RH, editors. Supercooled liquid, bulk glassy and nanocrystalline states of alloys. MRS proceedings, vol. 644. 2001. p. L10.7, http://dx.doi.org/10.1557/PROC-644-L10.7.
[61] Lund A, Schuh C. The Mohr-Coulomb criterion from unit shear processes in metallic glass. Intermetallics 2004;12(10–11):1159–65.
[62] Falk ML. Molecular-dynamics study of ductile and brittle fracture in model nanocrystalline solids. Phys Rev B 1999;60(10):7062.
[63] Shi Y, Falk ML. Does metallic glass have a backbone? The role of percolating short range order in strength and failure. Scripta Mater 2006;54(3):381–6.
[64] Shi Y, Falk ML. Strain localization and percolation of stable structure in amorphous solids. Phys Rev Lett 2005;95(9):095502.
[65] Sun L, Jiang MQ, Dai LH. Intrinsic correlation between dilatation and pressure sensitivity of plastic flow in metallic glasses. Scripta Mater 2010;63(9):945–8.
[66] Chen MW, Inoue A, Zhang W, Sakurai T. Extraordinary plasticity of ductile bulk metallic glasses. Phys Rev Lett 2006;96:245502–4.
[67] Heggen M, Spaepen F, Feuerbacher MJ. Creation and annihilation of free volume during homogeneous flow of a metallic glass. J Appl Phys 2005;97, 033506-1–033506-8.
[68] Inoue A, Zhang W, Tsurui T, Yavari AR, Greer AL. Unusual room-temperature compressive plasticity in nanocrystal-toughened bulk copper–zirconium glass. Philos Mag Lett 2005;85(5):221–9.
[69] Shen J, Wang G, Sun JF, Stachurski ZH, Yan C, Ye L, et al. Superplastic deformation behavior of $Zr_{41.25}Ti_{13.75}Ni_{10}Cu_{12.5}Be_{22.5}$ bulk metallic glass in the supercooled liquid region. Intermetallics 2005;13(1):79–85.
[70] Wang Q, Blandin JJ, Suery M, Van de Moortéle B, Pelletier JM. Homogeneous plastic flow of fully amorphous and partially crystallized $Zr_{41.2}Ti_{13.8}Cu_{12.5}Ni_{10}Be_{22.5}$ bulk metallic glass. J Mater Sci Technol 2003;19(6):557–60.
[71] Lee SC, Lee CM, Yang JW, Lee JC. Microstructural evolution of an elastostatically compressed amorphous alloy and its influence on the mechanical properties. Scripta Mater 2008;58:591–4.
[72] Ke HB, Wen P, Ping HL, Wang WH, Greer AL. Homogeneous deformation of metallic glass at room temperature reveals large dilatation. Scripta Mater 2011;64:966–9.
[73] Fujita T, Wang Z, Liu Y, Sheng H, Wang W, Chen M. Low temperature uniform plastic deformation of metallic glasses during elastic iteration. Acta Mater 2012;60:3741–7.
[74] Zhao K, Xia XX, Bai HY, Zhao DQ, Wang WH. Room temperature homogeneous flow in a bulk metallic glass with low glass transition temperature. Appl Phys Lett 2011;98(14):141913–23.
[75] Volkert CA, Donohue A, Spaepen F. Effect of sample size on deformation in amorphous metals. J Appl Phys 2008;103:083539.
[76] Guo H, Yan PF, Wang YB, Tan J, Zhang ZF, Sui ML, et al. Tensile ductility and necking of metallic glass. Nat Mater 2007;6(10):735–9.
[77] Spaepen F. Homogeneous flow of metallic glasses: a free volume perspective. Scripta Mater 2006;54:363–7.
[78] Li JCM. Mechanical properties of amorphous metals. Proceedings of the fourth international conference on rapidly quenched metals, vol. 2. Sendai, Japan: Japan Institute of Metals; 1982. p. 1335–40.